Assessment of potential impact of climate change on streamflow: a case study of the Brahmani River basin, India

Kumari Vandana, Adlul Islam, P. Parth Sarthi, Alok K. Sikka and Hemlata Kapil

ABSTRACT

The impact of future climate change on streamflow in the Brahmani River basin, India has been assessed using a distributed parameter hydrological model Precipitation Runoff Modelling System (PRMS) and multi-model ensemble climate change scenarios. The multi-model ensemble climate change scenarios were generated using the Hybrid-Delta ensemble method for A2, A1B, and B1 emission scenarios for three different future periods of the 2020s (2010–2039), 2050s (2040–2069) and 2080s (2070–2099). There is an increase in annual mean temperature in the range of 0.8–1.0, 1.5–2.0 and 2.0–3.3 °C during the 2020s, 2050s, and 2080s, respectively. Annual rainfall is projected to change in the range of −1.6–1.6, 1.6–3.1, and 4.8–8.1% during the 2020s, 2050s and 2080s, respectively. Simulation results indicated changes in annual streamflow in the range of −2.2–2.5, 2.4–4.7, and 7.3–12.6% during the 2020s, 2050s, and 2080s, respectively. Simulation results showed an increase in high flows and reduction in low flows, but the frequency of both high and low flow increases during future periods. The results of this work will be useful in developing a water management adaptation plan in the study basin.

Key words | climate change, high flow, hybrid-delta ensemble method, low flow, PRMS

Kumari Vandana (corresponding author)
P. Parth Sarthi
Centre for Environmental Sciences,
Central University South Bihar,
BIT Campus, P.O: B. V. College, 800 014
Patna, India
E-mail: *vandanakmr05@gmail.com*

Adlul Islam
Hemlata Kapil
Natural Resource Management Division,
Indian Council of Agricultural Research,
KAB-II, Pusa, New Delhi 110012,
India

Alok K. Sikka
IWMI Representative-India & Principal Researcher,
International Water Management Institute,
NASC Complex, Pusa, New Delhi 110012,
India

INTRODUCTION

Increase in temperature and changes in precipitation pattern due to global climate change are expected to alter regional hydrological conditions, affecting water resources availability and the discharge regime of rivers. Changes in amount, intensity and frequency of the precipitation will not only affect the magnitude of streamflow, but will also alter the intensity and frequency of occurrence of extreme events such as floods and droughts. This could have significant implications for water resource management (Kundzewicz *et al.* 2008). Changes in flow extremes under changing climate scenarios will have serious implications on design and regulations of water management structures. The assessment of possible impact of climate change on hydrological regimes has become imperative in recent years for ensuring appropriate water management strategies and developing suitable adaptation plans with due consideration of climate related risks in the planning process.

There are several studies dealing with the impact of projected climate change on basin hydrology and water resources availability (e.g. Christensen & Lettenmaier 2007; Raje *et al.* 2014; Ficklin *et al.* 2016). The magnitude and direction of climate change impact depends on the catchment, hydrological model and climate change scenarios used, and the flow index examined (Boorman & Sefton 1997). Studies focusing on different river basins in India have projected a varied magnitude of changes in streamflow in different river basins (Islam *et al.* 2014). Based on the simulation studies conducted using the Soil and Water Assessment tool (SWAT) and PRECIS (Providing Regional Climates for Impacts Studies) regional climate

doi: 10.2166/wcc.2018.129

model (RCM) projections under A1B emission scenario, Gosain *et al.* (2011) reported an increase in rainfall and associated increase in water yield of the majority of the river basins of India for the period 2021–2050 and 2071–2098. Raneesh & Santosh (2011) reported a decrease in streamflow in the River Chaliyar, Kerala, India under the PRECIS projected climate change scenarios for A2 and B2 emission scenarios. Islam *et al.* (2012c) reported a 62% increase in annual streamflow under the combined effect of 4 °C temperature rise and 30% rainfall increase in the Brahmani River basin. Narsimlu *et al.* (2013) projected an increase in average annual streamflow of 16.4% for the mid-century (2021–2050) and a significant increase of 93.5% by the end-century (2071–2098) in the Upper Sind River basin using SWAT model and the PRECIS RCM generated climate change scenario. Raje *et al.* (2014) used the variable infiltration capacity (VIC) macro-scale hydrologic model to study large scale hydrologic impacts of climate change for Indian River basins and reported increases in runoff in most central Indian River basins, including Ganga, under future climate change scenarios. The spatial variations in runoff sensitivity to climatic changes suggest the need for basin specific climate change impact assessment to formulate appropriate water management adaptation plans and policies for local response.

Most hydrological studies use the impact approach for assessing the potential impact of climate change on hydrology and water resources at the basin or watershed scale. The impact approach generally involves: (i) selection of suitable hydrological model; (ii) calibration and validation of the hydrological model using observed hydro-climatic data; (ii) generation of climate change scenarios using different statistical/dynamical downscaling methods; (iii) simulation run of the hydrological model with baseline and future climatic data; and (iv) analyzing the impacts by comparing the results with the baseline simulation. Hydrological models provide a link between climate change and water yields through simulation of various hydrologic processes within the basin. Physically based, distributed parameter models that represent the spatial variability of land surface and climatic characteristics are more suitable for studying the hydrologic effects of land use change and climate variability for large basins (Andersen *et al.* 2001; Minville *et al.* 2008).

General circulation models (GCMs) are the primary source of data for climate change impact assessment studies. Climate change scenarios generated from the GCM outputs produce more realistic scenarios than hypothetical scenarios (Legesse *et al.* 2003). However, the scale mismatch between the coarse resolution of GCMs and fine resolution data requirements of hydrologic models is one of the major constraints in climate change impacts assessments on water resources at the basin level. Therefore, spatial downscaling to scales more representative of the local area of interest is required for regional impact assessment studies (Christensen & Lettenmaier 2007). Parth Sarthi *et al.* (2012) suggested that spatial distribution of June–July–August (JJA) rainfall during 1961–1990 in CCSM3, ECHAM5 and MIROC (Hires) models seem to be close to the observed rainfall of India Meteorological Department (IMD) and show less biasness, especially over regions of Central Northeast India which includes the study area. Since each climate model has its own uncertainty, impact assessment based on projection of only one GCM may result in contrasting streamflow projections and could lead to inappropriate planning and adaptation responses (Wilby & Harris 2006; Kundzewicz *et al.* 2008; Mujumdar & Ghosh 2008). The use of climate projections from multiple GCMs and greenhouse gas emission scenarios (GHGES) are generally preferred to address the uncertainty linked to GCMs and GHGES (Christensen & Lettenmaier 2007; Maurer 2007; Elshamy *et al.* 2009). However, the use of multiple models with multiple scenarios leads to a number of realizations, and may not be useful for deriving adaptation strategies (Mujumdar & Ghosh 2008). To circumvent this problem, several authors have used an ensemble of multiple GCMs and emission scenarios to reduce the uncertainty associated with individual GCM projections (Raff *et al.* 2009; Islam *et al.* 2012a, 2012b; Ma *et al.* 2017).

The Brahmani River is one of the important inter-state east flowing rivers of peninsular India. The river flows through the states of Jharkhand, Chhattisgarh and Odisha before it outfalls into the Bay of Bengal. The delta of the Brahmani River basin is likely to experience severe flooding under the changing climate scenarios (Gosain *et al.* 2006; Prabhakar & Shaw 2008). The Brahmani River is the main source of irrigation water in the state of Odisha, and is likely to experience an increase in moderate drought development during 2021–2050 (Gosain *et al.*

2011). The previous studies on climate change impact on water resources availability in the Brahmani River basin is based on either hypothetical scenarios (Islam *et al.* 2012c) or the selected GCM/RCM scenario (Gosain *et al.* 2006, 2011). Further, most of the climate change impact assessment studies for Indian River basins have been conducted using the SWAT model (e.g. Gosain *et al.* 2006, 2011; Mishra & Lilhare 2016). The present study investigates the impact of climate change on flow regime in the Brahmani River basin using an offline hydrological model and multi-model ensemble climate change scenarios. In this study, the Precipitation Runoff Modelling Systems (PRMS) was used to simulate basin hydrology for three different future periods of the 2020s (2010–2039), 2050s (2040–2069) and 2080s (2070–2099). Multi-model ensemble climate change scenarios were generated using Coupled Model Inter-comparison Project phase-3's (CMIP3) 16 GCMs projections under three different emission scenarios of A2 (high emission), A1B (medium emission), and B1 (low emission). Results were analyzed in terms of changes in mean monthly, seasonal and annual streamflow. Changes were computed against the baseline scenario of no changes in rainfall and temperature. Further, changes in magnitude and frequency of high and low flow were also analyzed to study the effect of climate change on hydrological extremes.

MATERIALS AND METHODS

Study area

The Brahmani River basin is located in the eastern part of India and is situated within the latitudes of 20°30′10″ and 23°36′42″N and the longitudes of 83°52′55″and 87°00′38″E (Figure 1). The basin, with a total catchment area of 39,313 km^2, has four distinct sub-basins, namely, Tilga, Jaraikela, Gomlai and Jenapur. It receives an average annual rainfall of 1305 mm, with most of the rain occurring during the 4 months (June–October) of the southwest monsoon season. The maximum temperature reaches as high as 47 °C in summer and the minimum temperature drops to 4 °C in winter. The basin is the main source of water supplies for different towns and industries, and for irrigation in the state of Odisha (India). With population growth and economic development in the region, water resources availability both in terms of quantity and quality of water is a major cause of concern. Rain-fed agriculture is predominant in the region,

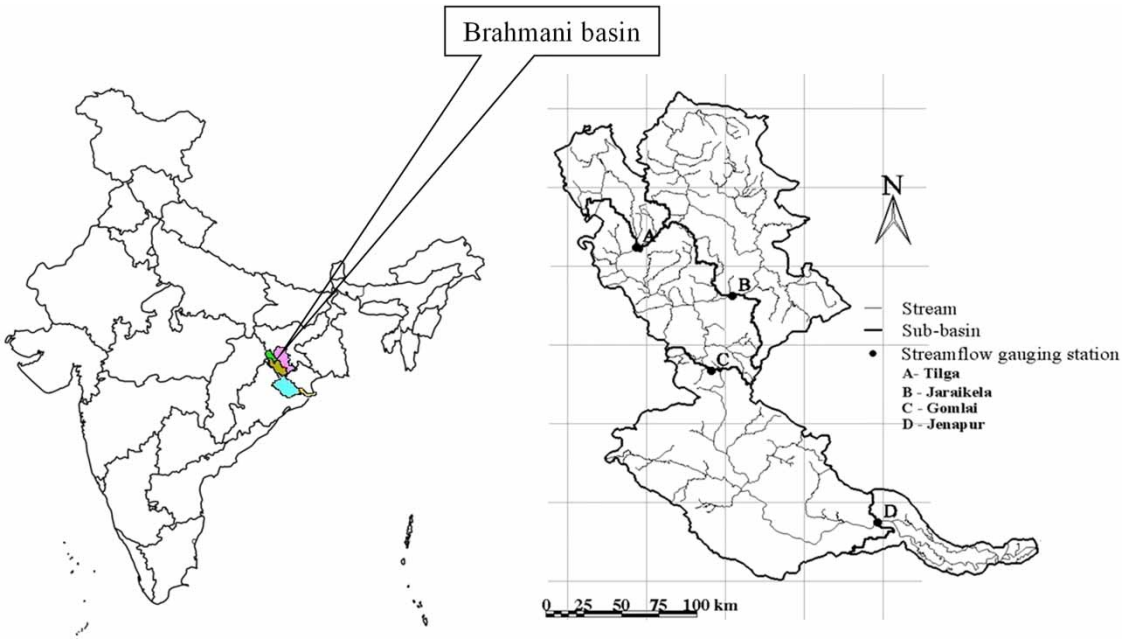

Figure 1 | Location map of the Brahmani River basin.

except in the lower deltaic parts where irrigation plays a major role. Flood is a recurring feature in the delta region. The problem of water scarcity as well as flood-like situations may be further aggravated under the changing climate scenarios. Thus, understanding the impact of future climate change in basin hydrology is essential for developing suitable water management adaptation plans for addressing the water resources problems in the area.

Data

Daily streamflow and rainfall data for the period 1979–2012 from four stream gauging stations, namely Tilga, Jaraikela, Gomlai and Jenapur, were collected from the Central Water Commission (CWC), Bhubaneswar (India). Daily minimum and maximum temperature data and daily rainfall data (1971–2005) at $0.5 \times 0.5^{\circ}$ spatial resolutions (Rajeevan & Bhate 2009) were also obtained from the IMD, Pune. The catchment area map was from the CWC. Soil and land use map of the study area were collected from the National Bureau of Soil Survey & Land Use Planning (NBSS & LUP). Toposheets of 1:250,000 scale with Universal Transverse Mercator (UTM) projection and 60 m contour intervals were used for generation of a digital elevation model (DEM) and delineation of basin into sub-basin and hydrological response units (HRUs) (Islam *et al.* 2012c).

The Bias Corrected and Spatially Downscaled (BCSD) global climate model output at $0.5 \times 0.5^{\circ}$ grid from the World Climate Research Programme's (WCRP's) Coupled Model Inter-comparison Project phase 3 (CMIP3) multi-model dataset (Meehl *et al.* 2007) for the period 1950–2099 were obtained from www.engr.scu.edu/~emaurer/global_data/ for the generation of climate change scenarios. These data were downscaled as described by Maurer *et al.* (2009) using the bias-correction/spatial downscaling method (Wood *et al.* 2004) to a 0.5° grid, based on the 1950–1999 gridded observed data (Adam & Lettenmaier 2003). In this study, projected changes in rainfall and temperature for 16 different GCMs and three different emission scenarios (A2, A1B and B1) were used (Table 1). The Special Report on Emission Scenarios (SRES) of A2, A1B and B1 represents high, medium and low emission scenarios, respectively.

Table 1 | List of global climate model projections used

	Modeling group, country	IPCC model ID
1	Bjerknes Centre for Climate Research, Norway	BCCR-BCM2.0
2	Canadian Centre for Climate Modeling & Analysis, Canada	CGCM3.1 (T47)
3	Meteo-France/Centre National de Recherches Meteorologiques, France	CNRM-CM3
4	CSIRO Atmospheric Research, Australia	CSIRO-Mk3.0
5	US Dept. of Commerce/NOAA/Geophysical Fluid Dynamics Laboratory, USA	GFDL-CM2.0
6	US Dept. of Commerce/NOAA/Geophysical Fluid Dynamics Laboratory, USA	GFDL-CM2.1
7	NASA/Goddard Institute for Space Studies, USA	GISS-ER
8	Institute for Numerical Mathematics, Russia	INM-CM3.0
9	Institute Pierre Simon Laplace, France	IPSL-CM4
10	Center for Climate System Research (The University of Tokyo), National Institute for Environmental Studies, and Frontier Research Center for Global Change (JAMSTEC), Japan	MIROC3.2 (medres)
11	Meteorological Institute of the University of Bonn, Germany; Meteorological Research Institute of KMA, Korea	ECHO-G
12	Max Planck Institute for Meteorology, Germany	ECHAM5/ MPI-OM
13	Meteorological Research Institute, Japan	MRI-CGCM2.3.2
14	National Center for Atmospheric Research, USA	CCSM3
15	National Center for Atmospheric Research, USA	PCM
16	Hadley Centre for Climate Prediction and Research/Met Office, UK	UKMO-HadCM3

Hydrological modelling system – PRMS

The US Geological Survey's Precipitation Runoff Modelling System (Leavesley *et al.* 1983, 2002) was selected for this study. This model has been widely used to study the effect of land use and climate change scenarios on streamflow (Hay *et al.* 2006; Qi *et al.* 2009; Islam *et al.* 2012c). PRMS is a physical process based, distributed parameter modelling system designed to analyze the effect of precipitation, climate, and land use on streamflow and other general basin hydrology (Leavesley *et al.* 1983). Distributed parameter capabilities of the model are provided by partitioning the basin into hydrologic response units (HRUs). HRUs are hydrologically homogenous units based on the characteristics such as slope, elevation, aspect, vegetation type, soil type, and precipitation distribution. A water balance is computed daily for each HRU and the sum of the responses of all HRUs weighted on a unit-area basis produces the daily watershed response. The model operates on a daily time step as well as at the storm mode. In this study, the daily time step is used to simulate streamflow at the basin outlet. Daily values of precipitation and minimum and maximum temperature of 16 grid points (Figure 1) located within the basin were used as input to the model. The XYZ method (xyz_dist module) distributes daily observed precipitation and maximum and minimum temperature data from 16 grid points to each HRU based on the longitude (x), latitude (y), and elevation (z) information using the multiple linear regression (MLR) equation (Hay *et al.* 2000, 2006).

In PRMS, a basin is conceptualised as a series of reservoirs, namely, the impervious-zone reservoir, the soil-zone reservoir, the unsaturated subsurface reservoir and the groundwater reservoir (Figure 2). Outputs of these reservoirs produce the total watershed response. The impervious-zone reservoir loses water as evaporation at a rate of potential evaporation. Soil water processes include infiltration, evaporation, plant water uptake, lateral flow, and percolation to lower layers. The depth of the soil zone is determined by the average root zone depth of the predominant vegetation type in the HRU. The soil zone is divided into two layers. The upper zone loses water through evaporation and plant transpiration and the lower zone loses only through transpiration. Three different procedures namely,

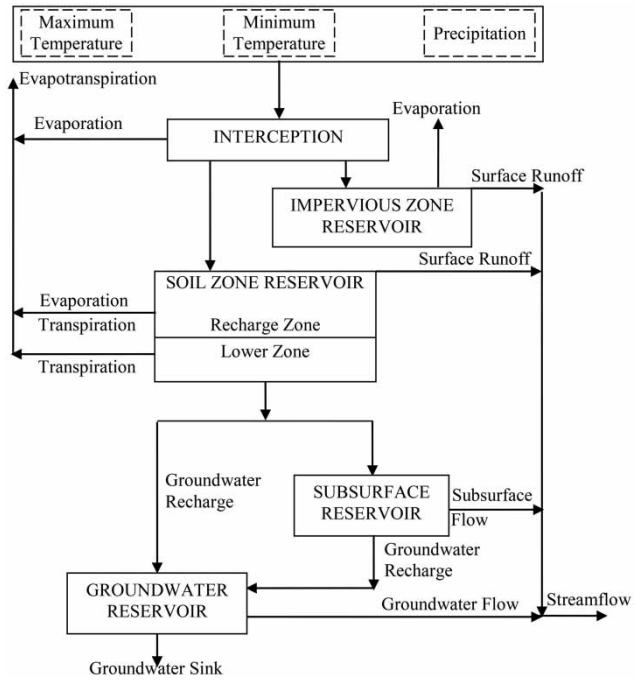

Figure 2 | Conceptual schematic diagram of the Precipitation Runoff Modeling System (adopted from Leavesley *et al.* 1983).

pan-evaporation, the Hamon method and the Jensen–Haise method are available for estimation of potential evapotranspiration (PET).

Net rainfall, defined as the difference of rainfall and vegetation canopy interception, is the source of moisture in the soil zone. Interception is computed as a function of canopy cover density and the storage available in the predominant vegetation type of the HRU. The volume of water infiltrating the soil zone is a function of soil characteristics, antecedent soil moisture conditions, and storm size. The surface runoff is computed using the contributing-area concept, whereby the percentage of a hydrologic response unit contributing to the surface runoff is computed as a linear function of antecedent soil moisture and net rainfall amount. Infiltration in excess of field capacity of the soil zone, after fulfilling the evaporative demand, is routed to lower layers. Repartitioning of this excess water between the subsurface and groundwater reservoirs is done using a coefficient, calibrated against measured streamflow data.

The subsurface storage behaves as a linear or nonlinear reservoir, and receives water from the soil zone when the field capacity is exceeded by infiltration. Subsurface flow (interflow) is determined as a function of the recharge rate

coefficient and the volume of water stored in the subsurface reservoir. The groundwater system is conceptualised as a linear reservoir and receives water from the soil zone and the subsurface reservoir. It is the source of all the base flow. Part of the groundwater is lost through deep percolation (seepage) to points beyond the area of interest. The sum of surface runoff, subsurface interflow and base flow is the daily total streamflow from the basin outlet. Different equations and approaches used for the computation of water balance components are described in Leavesley *et al.* (1983).

Model set-up

For hydrological modelling using PRMS, the DEM was developed with 30 m spatial resolution. The elevation and slope of basin varied between 28–1159 m and 0.28–20.5%, respectively. The elevation layer was sliced into three classes (Figure 3(a)) representing hilly (>800 m), plateau (400–800 m), and plain region (<400 m). Hilly, plateau and plain regions comprise 3.1, 41.5 and 55.40% of the total catchment area, respectively. A thematic map of soil (Figure 3(b)) with six textural classes (clay, clay loam, loamy, loamy sand, sandy loam, silt loam) and land use map (Figure 3(c)) with four classes (cultivated land, forest, settlement areas, water bodies) were then generated. Sandy loam is the major soil type occupying 43.6% of the catchment area followed by loamy sand (22%), clay loam (15.6%), silt loam (13.9%), loamy (4.8%), and clay (0.1%) soil. Cultivated land (69.9%) is the major land use class followed by forest (27.73%) and settlement area (0.2%). The water bodies occupy 2.2% of the catchment area. By overlaying the elevation layer, soil layer and land-use layer, the basin was delineated into 66 spatially distributed HRUs. Different HRU parameters, such as area, mean and median elevation, slope, land-use and soil type of each HRU, were extracted for input to the PRMS model.

Calibration and validation of hydrological model

The PRMS model was calibrated and validated using observed daily meteorological data (rainfall, maximum and minimum temperature) and daily streamflow data for the water years 1980–1992. One year data for the period 1979–1980 was used as a model warm-up period. We used the automatic-calibration tool called LUCA (Let Us CAlibrate) for calibration and validation of the PRMS model. LUCA uses a multiple objective, stepwise, automated calibration strategy with the Shuffled Complex Evolution global search algorithm (Hay *et al.* 2006). Daily streamflow data were used to calibrate the annual water balance, daily runoff at the basin outlet, whereas estimated monthly PET data were used to optimize PRMS evapotranspiration related parameters. In the first step of the calibration procedure, the parameters (Table 2) controlling the computation of PET were optimized using mean monthly PET values as the calibration dataset with an objective to

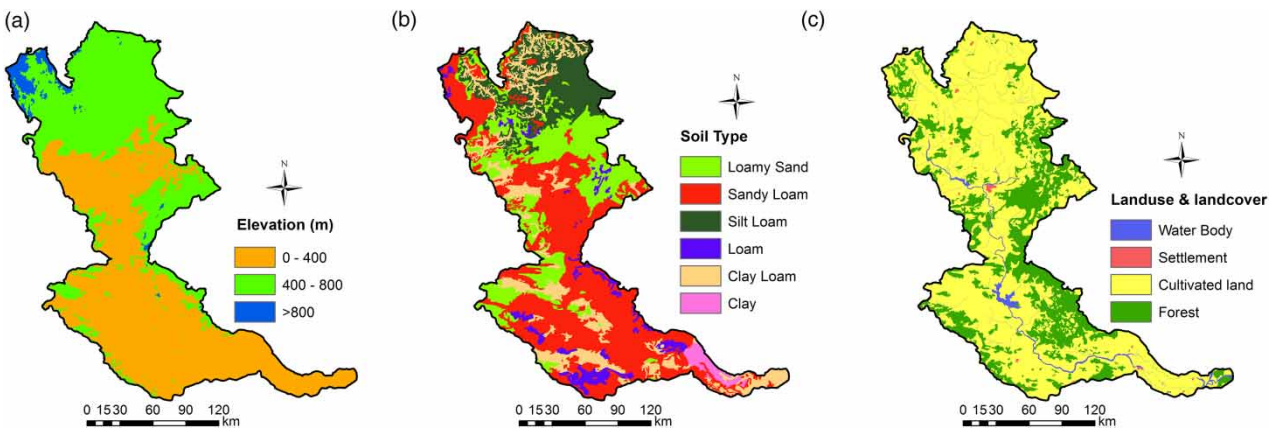

Figure 3 | Classified thematic maps of the Brahmani River basin.

Table 2 | Key PRMS calibration parameters with their description

Calibration objective	Objective function	Parameters	Description
Potential evapotranspiration	Sum of absolute difference	jh_coef	Coefficient used in Jensen–Haise potential ET computations
		jh_coef_ hru	Coefficient used in Jensen–Haise potential ET computations
Annual runoff volume	Normalized root mean square error	rain_adj	Monthly (January–December) factor to adjust measured precipitation on each HRU to account for differences in elevation, and so forth
		psta_freq_nuse	The subset of precipitation measurement stations used to determine if there is precipitation in the basin
		psta_nuse	The subset of precipitation measurement stations used in the distribution regression
Streamflow timing	Normalized root mean square error and Nash–Sutcliffe modeling efficiency	smidx_coef	Non-linear contributing area coefficient
		smidx_exp	Exponent in non-linear contributing area coefficient
		soil2gw_max	Maximum soil water excess that is routed directly to groundwater
		soil_moist_max	Maximum available water holding capacity of soil profile
		soil_rechr_max	Maximum available water holding capacity of recharge zone
		ssr2gw_exp	Non-linear coefficient in equation used to route soil-zone water to groundwater
		ssr2gw_rate	Linear coefficient in equation used to route soil-zone water to groundwater
		gwflow_coef	Linear groundwater discharge coefficient

minimize the sum of the absolute difference of observed and simulated PET. The second step in the calibration procedure adjusted the parameters to match the annual runoff volumes based on water year (June–May). The normalized root mean square error of observed and simulated streamflow was used as the objective function. In the last step of calibration procedure, PRMS parameters associated with daily streamflow timing, high and low flows (Table 2) were optimized with the objectives of minimizing the normalized root mean square error and maximizing the Nash–Sutcliffe modelling efficiency. Some other parameters, such as summer and winter cover density for major vegetation types on each HRU (covden_sum, coveden_win), and maximum possible area contributing to surface runoff (carea_max) were adjusted manually. For assessing the performance of the model in simulating streamflow, the classical hydrological model fit statistics, namely, Nash–Sutcliffe efficiency (NSE), percent bias (PBIAS), and ratio of the root mean square error to the standard deviation of measured data (RSR), and the coefficient of determination (R^2), were computed. For judging the model performance, the performance rating suggested by Moriasi *et al.* (2007) and Parajuli (2010) were used (Table 3).

Generation of climate change scenarios

The most commonly used method for climate change scenario generation is the 'delta change' or 'perturbation' method (Ragab & Prudhomme 2002). In this method differences between (or the ratio of) the control and future climate simulations are applied to historical observations by simply adding (or multiplying) the change factor to observed temperature (precipitation) data. This method is based on the assumptions that the biases of the GCM are similar during the baseline and the future period; and the temporal variability of the observed climate variables during the baseline period is maintained in the future simulated series (Khoi & Suetsugi 2012). The Hybrid-Delta (HD) ensemble method (Hamlet *et al.* 2010; Islam *et al.* 2012a, 2012b; Tohver *et al.* 2014), which considers inter-annual variability for each month, was used in this study. The hybrid delta method is similar to the Delta change method, but applies a different scaling factor to each month of the historic time series based on where it falls in the probability distribution of monthly values (Dickerson-Lange & Mitchell 2014). In this method, BCSD monthly GCM data were disaggregated into individual calendar

Table 3 | Performance rating of hydrological models for recommended statistics at monthly time step

	Moriasi *et al.* (2007)			Parajuli (2010)
Performance rating	**RSR**	**NSE**	**PBIAS %**	**R^2 value**
Excellent	–	–	–	>0.90
Very good	$0.00 \leq RSR \leq 0.5$	$0.75 \leq NSE \leq 1.00$	$\|PBIAS\| < 10$	0.75–0.89
Good	$0.5 < RSR \leq 0.6$	$0.65 < NSE \leq 0.75$	$10 < \|PBIAS\| \leq 15$	0.50–0.74
Satisfactory	$0.6 < RSR \leq 0.7$	$0.5 < NSE \leq 0.65$	$15 < \|PBIAS\| \leq 25$	0.25–0.49 (Fair)
Unsatisfactory	$RSR > 0.7$	$NSE < 0.5$	$\|PBIAS\| > 25$	0–0.24 (Poor)

months. Then a cumulative distribution function (CDF) for each of the months was developed for historical (1950–1999) and future time periods (2020s, 2050s, and 2080s). Similarly, the CDFs for the observed time series data (1971–1999) were also developed. With the CDFs, quantile mapping (Wood *et al.* 2002) was applied to re-map the observations onto the bias-corrected GCM data for each month to obtain the historic and future GCM projected rainfall and temperature data corresponding to the non-exceedance probability of observed data. It is to be noted here that quantile mapping was not applied for bias correcting GCM simulation to match observations; rather it was applied to re-map the observations onto the bias-corrected GCM data. For example, for a given observed temperature data for a given month, non-exceedance probability was first computed from the observed CDF of that month. Corresponding to this non-exceedance probability level, the historical and future temperature values from their respective CDFs were then obtained. The difference between the future and historical temperature values was then computed to obtain the change factor. In this way the change factor corresponding to all the observed values for a given month is computed. This process is repeated for all the 12 months. Thus, this method allowed for consideration of inter-annual variability for each month. A detailed description of the hybrid delta ensemble method is provided in Tohver *et al.* (2014). Using the above method, three multi-model ensemble climate change scenarios, namely: (i) ensemble of 16 projections representing the lower (B1) emission path; (ii) ensemble of 16 projections representing the middle (A1B) emission path; and (iii) ensemble of 16 projections representing the higher (A2) emission path were generated. For simulating the impact of projected climate change, the projected changes in precipitation and temperature were superimposed on the observed baseline data series (1971–1999). Results were analysed for all the three multi-model ensemble climate change scenarios and future periods separately to assess the climate change impact on streamflow in the basin.

RESULTS AND DISCUSSION

Calibration and validation of PRMS model

Calibration of the PRMS model by matching the observed and simulated streamflow for the period 1980–1986 showed a good agreement between observed and simulated streamflow (Figure 4). In general, the model simulated the trend of hydrograph and its variability reasonably well. As shown in Figure 4, the model could not capture some of the peak flow events during both the calibration and validation periods, and low flows during the validation period. The underestimation of daily streamflow for large peaks, occurring primarily during July–August, may be attributed to underestimation of areal rainfall in such a large basin as a local amount of rainfall may vary greatly across the basin. Based on the values of NSE, PBIAS, RSR and R^2 (Table 4), the model performance could be rated as 'very good' (Table 3) both on a daily and monthly timescale during the calibration period. The Nash–Sutcliffe modeling efficiency, which evaluates model error in relation to data variability, was found to be 0.95 and 0.80 at the monthly and daily timescale, respectively. During the calibration period, the RSR and PBAIS values remained less than 0.03 and 2.78, respectively, on a monthly as well as daily time scale. The coefficient of determination

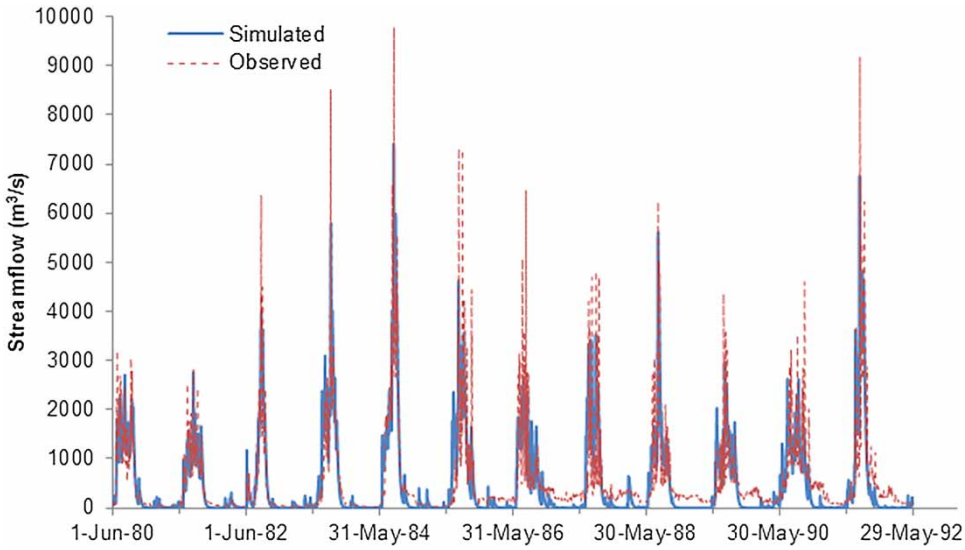

Figure 4 | Observed and simulated streamflow hydrograph during calibration and validation periods.

Table 4 | Model performance statistics during calibration and validation periods

	Calibration period (1980–1986)		Validation period (1986–1992)	
	Monthly	Daily	Monthly	Daily
R^2	0.95	0.80	0.87	0.64
NSE	0.95	0.80	0.79	0.59
RSR	0.03	0.01	0.05	0.01
PBIAS	2.78	2.71	15.93	15.80

(R^2) also remained greater than 0.8 for monthly as well as daily streamflow, and hence, the performance of the model can be rated as 'very good' (Parajuli 2010). As expected, the values of R^2, NSE, PBIAS, and RSR were slightly lower on the daily time scale, but it remained within the acceptable range of 'very good' criteria (Moriasi *et al.* 2007; Parajuli 2010). Although the performance ratings given in Table 3 are on a monthly time scale, they can be used with appropriate changes on a daily time scale (Moriasi *et al.* 2007).

Based on the monthly streamflow, the R^2, NSE, RSR and PBIAS were estimated as 0.87, 0.79, 0.05 and 15.93 indicating a very good model performance during the validation period. However, on the daily time scale the R^2, NSE, RSR and PBIAS were estimated as 0.64, 0.59, 0.01 and 15.80, respectively, and hence the model performance could be rated as 'good' to 'satisfactory'. The relatively lower performance of the model during the validation period may be attributed to an alteration in natural flow due to the presence of the multipurpose dam (Regnali dam) upstream of Jenapur gauging station, which has been operational since 1985 (Croke *et al.* 2011). Although the presence of a large dam in the Jenapur catchment complicates the hydrological response as the behavior of such dams is not captured by most of the hydrological models, the catchment was included in the study because modeling such catchments is necessary for water resource management. Mishra & Lilhare (2016) selected gauging stations located at the upstream region of the basin that are least affected by the presence of dams and reservoirs. Overall the PRMS model was able to capture the hydrological characteristics of the basin, and to reproduce the streamflow pattern and overall water balance reasonably well within an acceptable level of accuracy. Thus, the model can be applied for assessing changes in streamflow based on long term simulations under the projected climate change scenarios.

Climate change scenarios

Temperature variability

As shown in Figure 5, there is an increase (relative to 1951–1999) in annual mean temperature (Tmean) in the basin during all the three future periods of 2020s, 2050s, and 2080s. The increase in mean annual mean temperature

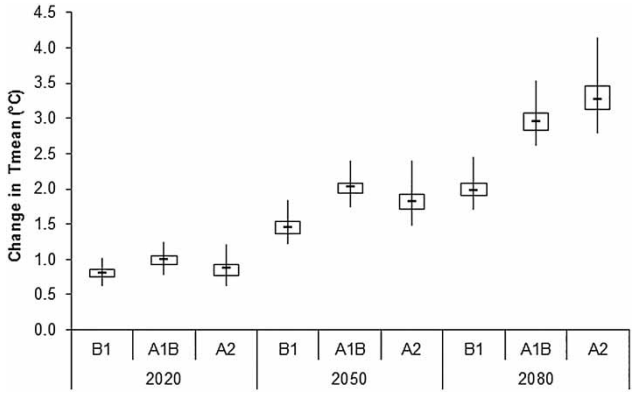

Figure 5 | Projected changes in annual mean temperature under different climate change scenarios during the 2020s, 2050s and 2080s.

under different emission scenarios varied in the range of 0.8–1.0, 1.5–2.0 and 2.0–3.3 °C during the 2020s, 2050s and 2080s, respectively. Although the range (differences in maximum and minimum increase) increased from ensembles of B1 projections to ensembles of A2 projections, the increase in median as well as average value of the mean temperature is greater under the A1B emission scenario as compared to the A2 emission scenario during the 2020s and 2050s. During the 2080s, the ensemble of GCM projections for A2 emission scenario resulted in a maximum increase in the mean temperature with an average increase of 3.3 °C. Monthly analysis showed an increase in the mean temperature during different months of the year in the range of 0.7–1.3, 1.2–2.5, and 1.7–4.0 °C during the 2020s, 2050s, and 2080s, respectively, under different emission scenarios (Table 5). The increase in mean temperature (Tmean) is at a maximum during the months of January–March whereas it is at a minimum during June–August. The increase in mean temperature during different months is likely to increase the evapotranspiration demand, affecting the soil moisture availability, and flow regimes in the basin.

Changes in rainfall

In general there is an increase in annual rainfall, though it is less than 10% in the basin during all three future periods. The changes in annual rainfall varied in the range of −1.6–1.6, 1.6–3.1, and 4.8–8.1% during the 2020s, 2050s and 2080s, respectively (Figure 6(a)). Monthly analyses showed large

Table 5 | Projected changes in mean temperature (°C) under different climate change scenarios

	2020s (2010–2039)			2050s (2040–2069)			2080s (2070–2099)		
Months	**B1**	**A1B**	**A2**	**B1**	**A1B**	**A2**	**B1**	**A1B**	**A2**
Jan	0.9	1.2	0.9	1.8	2.3	2.0	2.4	3.4	3.9
Feb	1.0	1.3	1.1	1.8	2.5	2.2	2.4	3.5	4.0
Mar	0.9	1.2	1.0	1.7	2.3	2.1	2.4	3.4	4.0
Apr	0.8	1.0	1.0	1.5	2.2	1.9	2.1	3.2	3.6
May	0.8	1.0	0.8	1.3	2.1	1.8	1.9	3.0	3.1
Jun	0.7	0.9	0.7	1.2	1.8	1.5	1.8	2.7	2.9
Jul	0.7	0.9	0.9	1.2	1.7	1.7	1.7	2.6	2.8
Aug	0.8	0.9	0.9	1.3	1.8	1.7	1.7	2.6	2.9
Sep	0.8	0.9	0.8	1.2	1.8	1.6	1.8	2.6	2.9
Oct	0.7	0.8	0.8	1.3	1.9	1.7	1.8	2.7	3.1
Nov	0.8	0.8	0.8	1.4	1.9	1.8	1.9	2.9	3.2
Dec	0.9	0.9	0.8	1.6	2.1	2.0	2.1	3.1	3.5

variations in the projected rainfall under different scenarios for all three future periods (Figure 7). The mean monthly rainfall changes under different emission scenarios varied in the

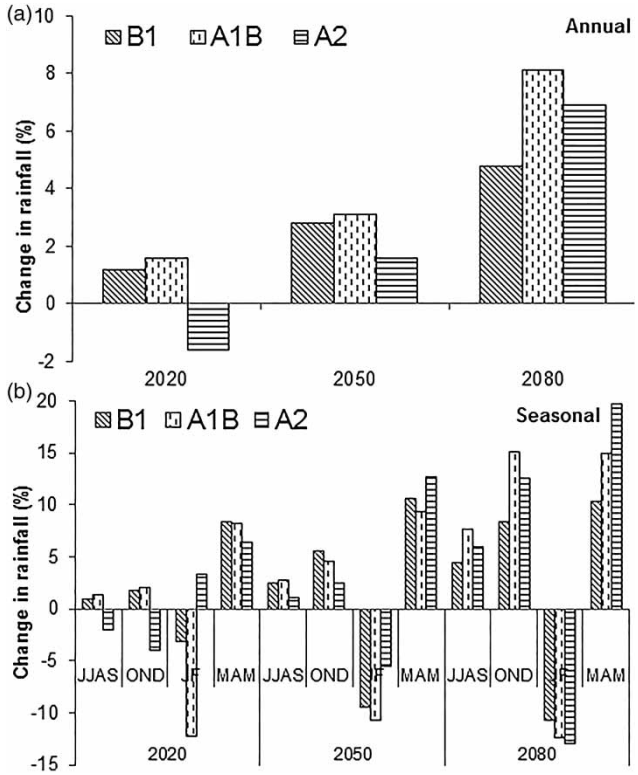

Figure 6 | Projected changes in annual and seasonal rainfall under different climate change scenarios during the 2020s, 2050s, and 2080s.

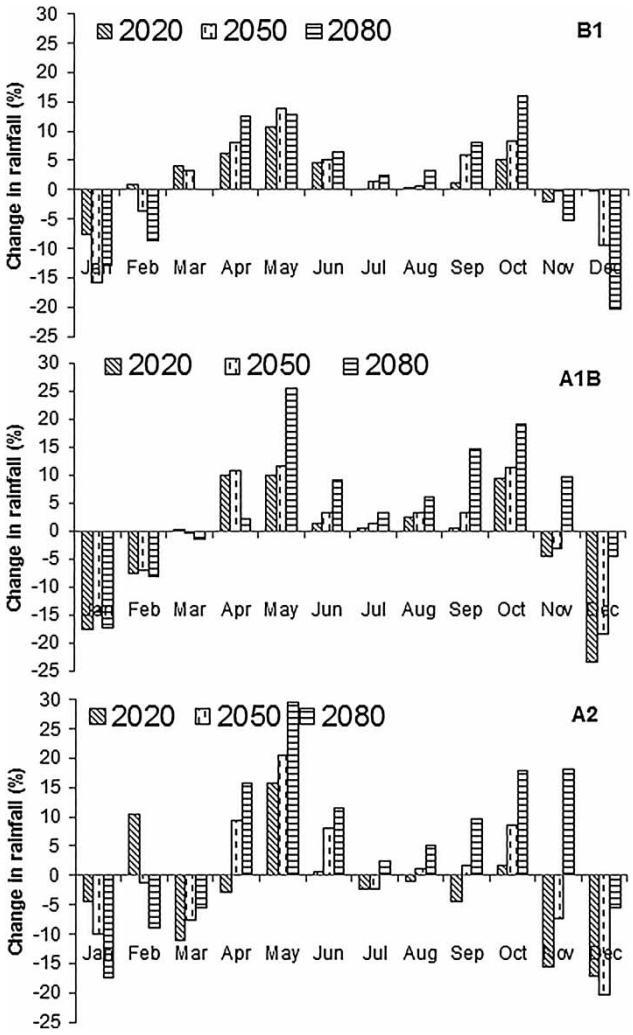

Figure 7 | Projected changes in monthly rainfall under different climate change scenarios during the 2020s, 2050s, and 2080s.

range of −23.4–15.7, −20.3–20.6, and −20.4–29.5% during the 2020s, 2050s, and 2080s, respectively. There is a decrease in rainfall during December and January months for all three emission scenarios and during all three future periods. Seasonally, there is an increase in rainfall during the monsoon (June–September) and post-monsoon (October–December) period under all three emission scenarios and future periods, except under A2 emission scenario during the 2020s (Figure 6(b)). The increase in rainfall during the monsoon season varied in the range of −2–1.4, 1.1–2.8, and 4.5–7.6% during the 2020s, 2050s, and 2080s, respectively. Similar to the monsoon and post-monsoon season, there is also an increase in pre-monsoon (March–May) rainfall under all three emission scenarios and future periods. The increase in rainfall is at a maximum during the pre-monsoon season, followed by post-monsoon and monsoon season rainfall. The increase in pre-monsoon rainfall varied in the range of 6.4–8.3, 9.3–12.7 and 10.3–19.7% during the 2020s, 2050s, and 2080s, respectively. During the winter season (January–February), there is a decrease in rainfall under all the three emission scenarios and future periods, except during the 2020s under A2 emission scenario when it recorded an increase of 3.3%. The decrease in rainfall during the winter season varied in the range of 3.1–12.3, 5.5–10.7 and 10.7–13.0% during the 2020s, 2050s, and 2080s, respectively. These changes in the rainfall pattern coupled with an increase in mean temperature in the basin will affect the water resources variability and flow regimes in the basin. The decrease in rainfall during the winter season is also likely to affect crop production in the absence of any supplemental irrigation.

Climate change impact on streamflow

Comparison of simulated streamflow for different time horizons (2020s, 2050s and 2080s) with the baseline period (no change in temperature and precipitation) showed an increase in streamflow for most of the projected climate change scenario. Changes in annual streamflow varied in the range of −2.2–2.5, 2.4–4.7 and 7.3–12.6% during the 2020s, 2050s and 2080s, respectively (Figure 8). The increase in annual streamflow is the maximum under the A1B emission scenario as compared to the B1 and A2 emission scenarios during all three future periods.

Analysis of seasonal streamflow showed an increase in streamflow during monsoon (JJAS), post-monsoon (OND) and pre-monsoon (MAM) seasons in all three future periods except during the 2020s under the A2 emission scenario. This decrease in streamflow under the A2 emission scenario is found to be 2.5 and 3.9% in monsoon and post-monsoon seasons, respectively, during the 2020s. During the monsoon season changes in streamflow varied in the range of −2.5–2.3, 1.8–4.2 and 6.6–11.4% during the 2020s, 2050s and 2080s, whereas during the post-monsoon period it varied in the range of −3.9–6.7, 6.9–10.5, and 16.8–27.8% during the future periods of the 2020s, 2050s and 2080s (Figure 8). During the winter season (JF), there is a decrease in streamflow during all three future periods and emission scenarios,

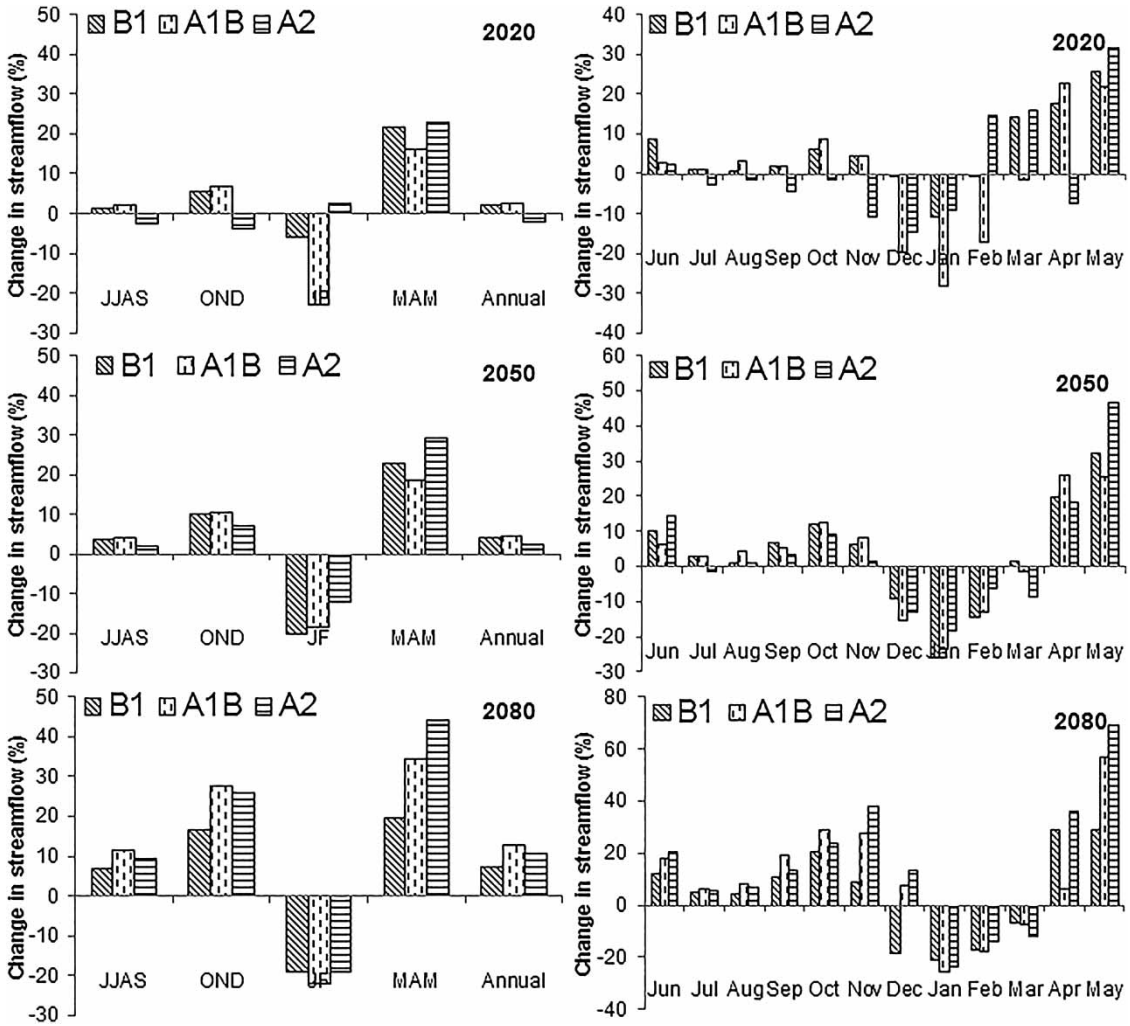

Figure 8 | Projected changes in monthly, seasonal and annual streamflow under different climate change scenarios during the 2020s, 2050s, and 2080s.

except during the 2020s under the A2 emission scenario. The decrease in streamflow during the winter season varied in the range of 5.9–22.8, 12.3–20.2, and 19.1–21.9% the during 2020s, 2050s, and 2080s, respectively. The pre-monsoon season recorded a maximum increase in streamflow and it varied in the range of 16.1–22.8, 18.7–29.0, and 19.7–44.3% during the 2020s, 2050s, and 2080s, respectively.

The analysis of monthly streamflow data also showed similar results. There is an increase in streamflow in most of the months, except during December–March, during all three future periods (Figure 8). In general, there is a decrease in streamflow in the months of December–March during the 2020s, 2050s and 2080s under all three emission scenarios. However, there is an increase in streamflow in the month of December under the A1B and A2 emission scenarios during the 2080s, and in the month of March under the B1 emission scenario during the 2050s. During the 2020s, there is an increase in streamflow in the month of March under the B1 and A2 emission scenarios and in the month of February under the A2 emission scenario. Further, the decrease in streamflow is the maximum during the month of January for all three future periods and emission scenarios, and the maximum decrease in streamflow is 28.2, 25.9, and 25.8% during the 2020s, 2050s and 2080s, respectively. During the monsoon months (June–September), there is an increase in streamflow under all three emission scenarios and during all

three future periods, except during the 2020s under the A2 emission scenario. Thus, there is temporal variability in streamflow changes in the basin, and changes in annual, seasonal and monthly streamflow are consistent with rainfall changes in the basin.

Climate change impact on high and low flows

The impact of climate change on flow regimes ranging from high to low flows can be represented by a flow duration curve (FDC) of the basin. A FDC graphically depicts the relationship between the frequency and magnitude of streamflow and gives an estimate of the percentage of time a given streamflow was equaled or exceeded over a historical period. FDCs have been used to study the effect of different climate change scenarios on streamflow (e.g. Wilby *et al.* 1994; Gosain *et al.* 2006; Gain *et al.* 2011). For the construction of FDCs, daily streamflow data were arranged in descending order of magnitude and probability of exceedance was computed using the Weibull's plotting position formula. FDCs were constructed for the baseline period and for each climate change scenarios for the future periods of the 2020s, 2050s and 2080s. A typical FDC for the 2080s (2070–2099) is shown in Figure 9. We used Q5 and Q10 as high flow indices, and Q90 and Q95 as low flow indices (Pyrce 2004) for evaluating changes in high and low flow characteristics in the basin. With high (Q5 or Q10) and low flow (Q95 or Q90) values from baseline FDC as the threshold values, numbers of streamflow events above ($Q5_{base}$ or $Q10_{base}$) or below ($Q95_{base}$ or $Q90_{base}$) the threshold values were computed to evaluate changes in frequencies of high and low flow events (Gellens & Roulin 1998).

The results presented in Table 6 indicate an increase in high flows under all the emission scenarios during all three future periods, except during the 2020s under the A2 emission scenario. The increase in high flows were in the range of 1.3–2.5, 1.2–4.5, and 6.8–12.1% during the 2020s, 2050s and 2080s, respectively. Further, the increase in high flow (Q5 and Q10) is the largest under the A1B emission scenario during all three future periods. Similar to the high flow magnitudes, the frequency of occurrences of high flow events (number of days flow exceeded $Q5_{base}$) also increased during all three future periods, except during the 2020s under the A2 emission scenario. The maximum increase in frequency of high flow events occurred during the 2080s and it varied in the range of 12.2–33.9%. During the 2020s and 2050s, the increase in frequencies of high flow events

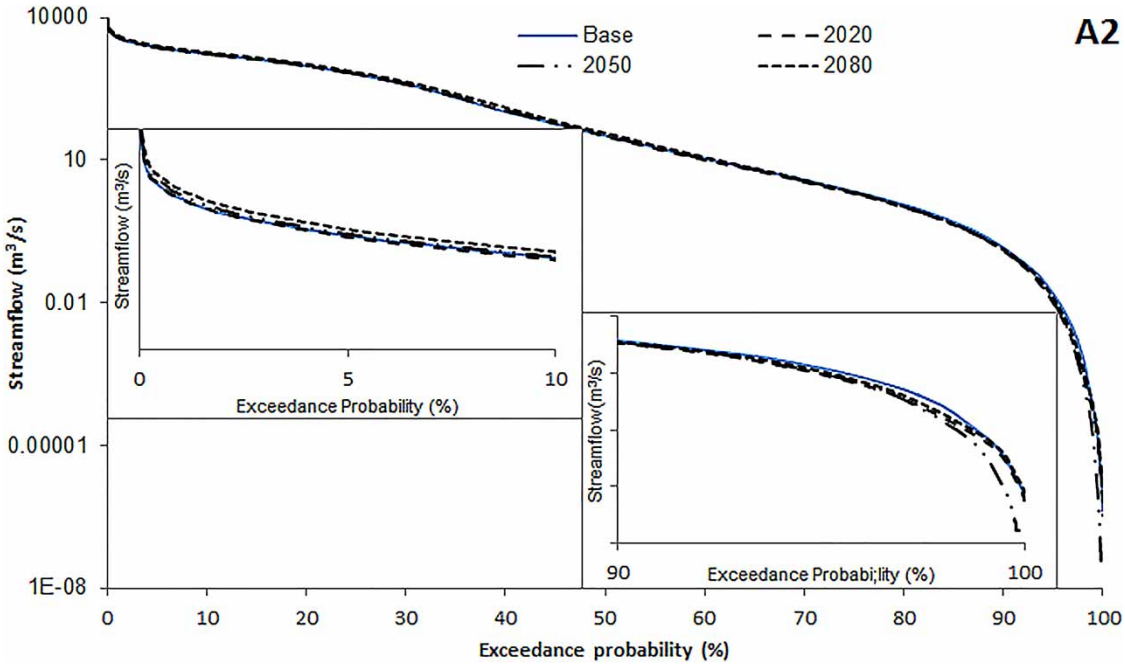

Figure 9 | Flow duration curve for the 2080s (2070–2099) under the A2 emission scenario.

Table 6 | Projected change in high and low flow magnitudes and frequencies at different probability levels

	Change in flow magnitude (%)			Change in flow frequency (%)		
Exceedance probability	**B1**	**A1B**	**A2**	**B1**	**A1B**	**A2**
2020s (2010–2039)						
5	1.3	2.5	–2.4	2.7	19.0	–5.1
10	1.5	2.1	–3.5	2.1	4.2	–5.3
90	–2.4	–12.9	–15.9	0.7	4.7	5.6
95	–7.0	–21.8	–36.7	2.0	7.0	12.1
2050s (2040–2069)						
5	3.0	4.5	1.7	8.4	11.2	4.9
10	4.0	4.5	1.2	7.1	7.5	2.4
90	–4.4	–11.6	–12.1	1.6	3.7	4.0
95	–13.1	–17.1	–31.0	3.9	5.9	10.2
2080s (2070–2099)						
5	6.8	12.1	9.7	17.6	33.9	25.6
10	7.4	11.5	9.2	12.2	19.9	15.3
90	–8.3	–5.0	–9.9	2.7	1.9	3.6
95	–24.1	–6.9	–20.4	7.0	2.0	6.1

varied in the range of 4.2–19.0 and 2.4–11.2%, respectively. Analysis of low flow (Q95 and Q90) indices indicated a decrease in the low flows in the basin during all three future periods under all the emission scenarios, and the decrease in low flows varied in the range of 2.4–36.7, 4.4–31.0, and 5.0–24.1% during the 2020s, 2050s, and 2080s, respectively. The decrease in low flows is greatest under the A2 emission scenario. It is also to be noted that the decrease in low flows is greater during the 2020s followed by the 2050s and 2080s. These results are also in confirmation of changes in annual streamflow in the basin as a greater increase in streamflow is projected during the 2080s, followed by the 2050s and 2020s, resulting in a decrease in low flows in the basin. There is also an increase in the frequency of low flow events and it varied in the range of 0.7–12.1, 1.6–10.2 and 1.9–7.0% during the 2020s, 2050s and 2080s, respectively. The FDCs thus revealed an increase in magnitude of flood flows while there is a reduction in magnitude of low flows under all scenarios during future periods. A comparison of relative changes in high and low flows indicated a greater change in low flows as compared to the high flows. This implies that greater attention may be needed to maintain environmental flows and developing drought management strategies in the basin.

The Brahmani basin plays a very important role in the socio-economic, agricultural and industrial development in the Odisha state. The water availability in the basin is dominated by monsoonal flows with low flows during the non-monsoon periods. As the flood as well as water scarcity during the non-monsoon period is a cause of concern in the basin, water harvesting and storing excess water during monsoon and post-monsoon season as an adaptation strategy will not only help to provide irrigation during *Rabi* (winter) season but will also help to attenuate the flood peak during the monsoon season. Although construction of Rengali dam has moderated the flood in the lower reach, the deltaic region still remains the most vulnerable, and is likely to be affected more under the projected climate change scenarios. With the urbanization, industrialization and agricultural intensification in the basin area, there is deterioration in the river water quality due to agricultural waste, fertilizer application, and discharge of industrial effluents into the river. The Bhitakanika mangrove ecosystem, which flourishes in the deltaic region of the basin, is facing serious threat due to deteriorating water quality and changes in flow regimes in the river. As low flow is projected to decrease in the future, environmental flow requirement needs careful consideration for maintaining the aquatic ecosystems, biodiversity of the mangroves in the delta region of the basin, and sustainable development of water resources in the basin.

The results presented in this study indicate plausible changes in the streamflow under the CMIP3 projected climate change scenarios. In this study, multi-model ensemble climate change scenarios have been used to account for the uncertainty associated GCM projections and emission scenarios. The analysis of monthly, seasonal and annual streamflow showed variation in the simulated streamflow under different multi-model ensemble climate change scenarios depending upon the emission scenarios. In general, there is an increase in annual streamflow in the basin and this increase in streamflow is consistent with an increase in rainfall in the basin. Although there is an increase in temperature in the basin, changes in rainfall have a greater effect on streamflow as compared to the change in temperature as the study basin is located in sub-humid climatic conditions (Islam *et al.* 2012c).

The hydrological simulation studies are subjected to uncertainties due to model structure and model parameterization (Poulin *et al.* 2011). For calibration of the model, a multiple objective, stepwise, automated calibration strategy with the Shuffled Complex Evolution global search algorithm has been used. During the calibration period, model performance was found to be very good on both daily and monthly time scales, and during the validation period the model was found to perform satisfactorily on a daily time scale. The study assumes that the calibrated hydrologic model will remain valid under future climate change scenarios too. It is also to be noted here that results presented in this study are in the form of relative changes. Niraula *et al.* (2015) reported that relative changes due to climate change predicted with the uncalibrated (UC), single outlet calibrated (OC) were not significantly different than that predicted with the spatially-calibrated (SC) model, and also indicated that model calibration is not necessary to determine the direction of change in streamflow due to LULC and climate change. Due to the uncertainty associated with the projected climate change scenarios, hydrologic model structure and model parameterization, there remains uncertainty in the projected changes in the streamflow. Nevertheless these results provide valuable information regarding changes in magnitude of streamflow under future climatic scenarios and could be used for developing suitable water management strategies.

It is worth mentioning here that the projected changes in streamflow are based on CMIP3 climate change projections, which are based on emission scenarios (A2, A1B, B1). The new-generation CMIP5 climate model projections, which are based on representative concentration pathways (RCPs), include a more complete representation of some physical processes and a finer spatial resolution for some models as compared to CMIP3 (Knutti & Sedlacek 2013). Sonali *et al.* (2017) reported an enhancement in skill of CMIP5 models compared to CMIP3 models in simulating the current seasonal cycles (monthly) of both maximum and minimum temperatures over India. However, Ramesh & Goswami (2014) reported that for Indian summer monsoon precipitation, there is no improvement in skill in CMIP5 projections as compared to CMIP3 projections in terms of reliability (confidence). While comparing the hydrologic impact using CMIP3 and CMIP5 projection, Ficklin *et al.* (2016) reported that projections of temperature, precipitation and streamflow timing are similar across the entire western United States (WUS), indicating robustness of the underlying climatic signals in both the CMIP3 and CMIP5 scenarios. However, in the Upper Colorado River basin (UCRB) CMIP5 based projections indicated an increase in future streamflow. For Brahmani River basin, Mishra & Lilhare (2016) suggested a comparatively higher increase in streamflow under CMIP5 projections as compared to the present study. The higher increase in streamflow under the CMIP5 projections may be due to a corresponding higher increase in rainfall as compared to the CMIP3 models. Mishra & Lilhare (2016) used five GCMs projections for RCP4.5 and RCP8.5 and used the SWAT model in their study, whereas in the present study 16 GCMs projections were used for generation of ensemble climate change scenarios and the PRMS model was used for hydrologic simulation. The result of impact assessment studies depends on the hydrological model(s) used, and climate change projection (GCM selected, number of GCMs used, downscaling method) used. Thus, it is important to study hydrologic impacts under CMIP3 and CMIP5 projections using similar climate change projections (GCMs form same modeling group, number of GCMs, etc.), hydrological model, and downscaling approach so as to assess the robustness of streamflow projections and reduce the uncertainty in streamflow projections. Such a comparison will help to assess whether CMIP3 projections are still useful or if there is a need to re-evaluate results obtained in many impact studies using CMIP5 projections.

CONCLUSIONS

Climate change is expected to alter the hydrological cycle, and will subsequently impact the spatial and temporal availability of water resources. This study investigates the impact of climate change on streamflow in the Brahmani River basin using multi-model ensemble climate change scenarios generated from 16 CMIP3 GCMs projections under three different emission scenarios of A2 (high emission), A1B (medium emission), and B1 (low emission). Hydrological simulation was carried out using a physically based distributed parameter model – the PRMS. Analysis of projected changes in mean temperature under different emission scenarios indicated an increase in annual mean temperature in

the range of 0.8–1.0, 1.5–2.0 and 2.0–3.3 °C during the 2020s, 2050s and 2080s, respectively, as compared to the baseline period of 1951–1999. In general, there is an increase in the annual rainfall in the basin and changes in rainfall varied in the range of –1.6–1.6, 1.6–3.1, and 4.8–8.1% during the 2020s, 2050s and 2080s, respectively. Simulation results indicated changes in annual streamflow in the range of –2.2–2.5, 2.4–4.7, and 7.3–12.6% during the 2020s, 2050s, and 2080s, respectively. Monthly analysis showed a large temporal variation in streamflow change with a decrease in streamflow during the winter months in all three future periods. The temporal variation in the streamflow in the basin suggests the need for developing different irrigation water management adaptation strategies for crop planning. Simulation results also showed an increase in magnitude of flood flows and a reduction in magnitude of low flows under all scenarios during future periods. There is also an increase in the frequency of high and low flow events in the basin. As an adaptation strategy, designing suitable water storage structures will be helpful in attenuating the flood peak during monsoon season and irrigating *Rabi* (winter) season crops. As the low flow is projected to decrease, the environmental flow requirements of the basin should be given due consideration in the planning and management of water resources in the basin.

ACKNOWLEDGEMENTS

This work was carried out under the network project 'National Innovations on Climate Resilient Agriculture (NICRA)' of the Indian Council of Agricultural Research (ICAR), New Delhi. The authors would like to thank the Central Water Commission, the India Meteorological Department and the ICAR-National Bureau of Soil Survey & Land Use Planning for providing necessary data for conducting this research work.

REFERENCES

Adam, J. C. & Lettenmaier, D. P. 2003 Adjustment of global gridded precipitation for systematic bias. *J. Geophys. Res.* **108**, 1–14.

Andersen, J., Refsgaard, J. C. & Jensen, K. H. 2001 Distributed hydrological modeling of the Senegal river basin: model construction and validation. *J. Hydrol.* **247** (3–4), 200–214.

Boorman, D. B. & Sefton, C. E. M. 1997 Recognising the uncertainty in the quantification of the effects of climate change on hydrological response. *Clim. Chang.* **35**, 415–434.

Christensen, N. S. & Lettenmaier, D. P. 2007 A multimodel ensemble approach to assessment of climate change impacts on the hydrology and water resources of the Colorado River Basin. *Hydrol. Earth Syst. Sci.* **11**, 1417–1434.

Croke, B., Islam, A., Ghosh, J. & Khan, M. A. 2011 Evaluation of approaches for estimation of rainfall and the unit hydrograph. *Hydrol. Res.* **42** (5), 372–385.

Dickerson-Lange, S. E. & Mitchell, R. 2014 Modeling the effects of climate change projections on streamflow in the Nooksack River basin, Northwest Washington. *Hydrol. Process.* **28** (20), 5236–5250.

Elshamy, M. E., Seierstad, I. A. & Sorteberg, A. 2009 Impacts of climate change on Blue Nile flows using bias-corrected GCM scenarios. *Hydrol. Earth Syst. Sci.* **13**, 551–565.

Ficklin, D. L., Letsinger, S. L., Stewart, I. T. & Maurer, E. P. 2016 Assessing differences in snowmelt-dependent hydrologic projections using CMIP3 and CMIP5 climate forcing data for the western United States. *Hydrol. Res.* **47**, 483–500.

Gain, A. K., Immerzeel, W. W., Sperna Weiland, F. C. & Bierkens, M. F. P. 2011 Impact of climate change on the stream flow of the lower Brahmaputra: trends in high and low flows based on discharge-weighted ensemble modelling. *Hydrol. Earth Syst. Sci.* **15**, 1537–1545.

Gellens, D. & Roulin, E. 1998 Streamflow response of Belgian catchments to IPCC climate change scenarios. *J. Hydrol.* **210** (1–4), 242–258.

Gosain, A. K., Rao, S. & Arora, A. 2011 Climate change impact assessment of water resources of India. *Curr. Sci.* **101** (3), 356–371.

Gosain, A. K., Rao, S. & Basuray, D. 2006 Climate change impact assessment on hydrology of Indian river basins. *Curr. Sci.* **90** (3), 346–353.

Hamlet, A. F., Salathe, E. P. & Carrasco, P. 2010 *Statistical Downscaling Techniques for Global Climate Model Simulations of Temperature and Precipitation with Application to Water Resources Planning Studies*. Available from: http://www.hydro.washington.edu/2860/report/.

Hay, L. E., Wilby, R. L. & Leavesley, G. H. 2000 A comparison of delta change and downscaled GCM scenarios for three mountainous basins in the United States. *J. Am. Water Resour. Assoc.* **36** (2), 387–397.

Hay, L. E., Leavesley, G. H., Clark, M. P., Markstrom, S. L., Viger, R. J. & Umemoto, M. 2006 Step-wise, multiple-objective calibration of a hydrologic model for a snowmelt-dominated basin. *J. Am. Water Resour. Assoc.* **42** (4), 877–890.

Islam, A., Ahuja, L. R., Garcia, L. A., Ma, L., Saseesndran, A. S. & Trout, T. J. 2012a Modeling the impact of climate change on irrigated corn production in the central great plains. *Agric. Water Manag.* **110**, 94–108.

Islam, A., Ahuja, L. R., Garcia, L. A., Ma, L. & Saseesndran, A. S. 2012b Modeling the effect of elevated CO_2 and climate change on potential evapotranspiration in the semi-arid central great plains. *Trans. ASABE* **55** (6), 2135–2146.

Islam, A., Sikka, A. K., Saha, B. & Singh, A. 2012c Streamflow response to climate change in the Brahmani River Basin, India. *Water Resour. Manag.* **26**, 1409–1424.

Islam, A., Shirsath, P. B., Kumar, S. N., Subhash, N., Sikka, A. K. & Aggarwal, P. K. 2014 Use of models in water management and food security under climate change scenarios in India. In: *Practical Applications of Agricultural System Models to Optimize the Use of Limited Water. Adv. Agric. Systems Modelling* (L. R. Ahuja, L. Ma & R. J. Lascano, eds). Vol. 5. ASA-SSSA-CSSA, Madison, WI, pp. 267–316.

Khoi, D. N. & Suetsugi, T. 2012 Hydrologic response to climate change: a case study for the Be River Catchment, Vietnam. *J. Water Clim. Change* **3** (3), 207–224.

Knutti, R. & Sedlacek, J. 2013 Robustness and uncertainties in the new CMIP5 climate model projections. *Nature Clim. Change* **3**, 369–373.

Kundzewicz, Z. W., Mata, L. J., Arnell, N. W., Döll, P., Jimenez, B., Miller, K., Oki, T., Sen, Z. & Shiklomanov, I. 2008 The implications of projected climate change for freshwater resources and their management. *Hydrol. Sci. J.* **53** (1), 3–10.

Leavesley, G. H., Lichty, R. W., Troutman, B. M. & Saindon, L. G. 1983 *Precipitation-Runoff Modeling System: User's Manual*. U.S. Geological Survey Investigation Report 83-4238. U.S. Geological Survey, Water Resources Division, Denver, Colorado, USA, 207 pp.

Leavesley, G. H., Markstrom, S. L., Restrepo, P. J. & Viger, R. J. 2002 A modular approach to addressing model design, scale, and parameter estimation issues in distributed hydrological modelling. *Hydrol. Process.* **16** (2), 173–187.

Legesse, D., Vallet-Coulomb, C. & Gasse, F. 2003 Hydrological response of a 11 catchment to climate and land use changes in Tropical Africa: case study of south central Ethiopia. *J. Hydrol.* **275**, 67–85.

Ma, L., Ahuja, L. R., Islam, A., Trout, T. J., Saseendran, S. A. & Malone, R. W. 2017 Modeling yield and biomass responses of maize cultivars to climate change under full and deficit irrigation. *Agric. Water Manag.* **180**, 88–98.

Maurer, E. P. 2007 Uncertainty in hydrologic impacts of climate change in the Sierra Nevada, California, under two emissions scenarios. *Clim. Change* **82**, 309–325.

Maurer, E. P., Adam, J. C. & Wood, A. W. 2009 Climate model based consensus on the hydrologic impacts of climate change to the Rio Lempa basin of Central America. *Hydrol. Earth Syst. Sci.* **13**, 183–194.

Meehl, G. A., Covey, C., Delworth, T., Latif, M., McAvaney, B., Mitchell, J. F. B., Stouffer, R. J. & Taylor, K. E. 2007 The WRCP CMIP3 multi-model dataset: a new era in climatic change research. *Bull. Am. Meteorol. Soc.* **88**, 1383–1394.

Minville, M., Brissette, F. & Leconte, R. 2008 Uncertainty of the impact of climate change on the hydrology of a nordic watershed. *J. Hydrol.* **358**, 70–83.

Mishra, V. & Lilhare, R. 2016 Hydrologic sensitivity of Indian sub-continental river basins to climate change. *Glob. Planet. Change* **139**, 78–96.

Moriasi, D. N., Arnold, J. G., Van Liew, M. W., Bingner, R. L., Harmel, R. D. & Veith, T. L. 2007 Model evaluation guidelines for systematic quantification of accuracy in watershed simulations. *Trans. ASABE* **50** (3), 885 – 900.

Mujumdar, P. P. & Ghosh, S. 2008 Modeling GCM and scenario uncertainty using a probabilistic approach: application to the Mahanadi River, India. *Water Resour. Res.* **44**, W06407.

Narsimlu, B., Gosain, A. K. & Chahar, B. R. 2013 Assessment of future climate change impacts on water resources of Upper Sind River Basin, India using SWAT model. *Water Resour. Manag.* **27**, 3647–3662.

Niraula, R., Meixner, T. & Norman, L. M. 2015 Determining the importance of model calibration for forecasting absolute/relative changes in streamflow from LULC and climate changes. *J. Hydrol.* **522**, 439–451.

Parajuli, P. B. 2010 Assessing sensitivity of hydrologic responses to climate change from forested watershed in Mississippi. *Hydrol. Process.* **24** (26), 3785–3797.

Parth Sarthi, P., Dash, S. K. & Mamgain, A. 2012 Possible characteristics of Indian summer monsoon under warmer climate. *Glob. Planet. Chang.* **92–93**, 17–29.

Poulin, A., Brissette, F., Leconte, R., Arsenault, R. & Malo, J. S. 2011 Uncertainty of hydrological modelling in climate change impact studies in a Canadian, snow-dominated river basin. *J. Hydrol.* **409**, 626–636.

Prabhakar, S. V. R. K. & Shaw, R. 2008 Climate change adaptation implications for drought risk mitigation: a perspective for India. *Clim. Chang.* **88** (2), 113–130.

Pyrce, R. S. 2004 *Hydrological Low Flow Indices and Their Uses*. WSC Report No. 04-2004. Watershed Science Centre, Peterborough, Ontario, 33 pp.

Qi, S., Sun, G., Wang, Y., McNulty, S. G. & Moore Myers, J. A. 2009 Streamflow response to climate and landuse changes in a coastal watershed in North Carolina. *Trans. ASABE* **52** (3), 739–749.

Raff, D. A., Pruitt, T. & Brekke, L. D. 2009 A framework for assessing flood frequency based on climate projection information. *Hydrol. Earth Syst. Sci.* **13**, 2119–2136.

Ragab, R. & Prudhomme, C. 2002 Climate change and water resources management in arid and semi-arid regions: prospective and challenges for 21st century. *Biosyst. Eng.* **81** (1), 3–34.

Raje, D., Priya, P. & Krishnan, R. 2014 Macroscale hydrological modelling approach for study of large scale hydrologic impacts under climate change in Indian river basins. *Hydrol. Process.* **28**, 1874–1889.

Rajeevan, M. & Bhate, J. 2009 A high resolution daily gridded rainfall dataset (1971–2005) for mesoscale meteorological studies. *Curr. Sci.* **96** (4), 558–562.

Ramesh, K. V. & Goswami, P. 2014 Assessing reliability of regional climate projections: the case of Indian monsoon. *Sci. Rep.* **4**, 4071.

Raneesh, K. Y. & Santosh, G. T. 2011 A study on the impact of climate change on streamflow at the watershed scale in the humid trophics. *Hydrolog. Sci. J.* **56** (6), 946–965.

Sonali, P., Nagesh Kumar, D. & Nanjundiah, R. S. 2017 Intercomparison of CMIP5 and CMIP3 simulations of the 20th century maximum and minimum temperatures over India and detection of climatic trends. *Theor. Appl. Climatol.* **128**, 465–489.

Tohver, I. M., Hamlet, A. F. & Lee, S. Y. 2014 Impacts of 21st century climate change on hydrologic extremes in the Pacific northwest region of North America. *J. Am. Water Resour. Assoc.* **50**, 1461–1476.

Wilby, R. L. & Harris, I. 2006 A framework for assessing uncertainties in climate change impacts: low-flow scenarios for the River Thames, UK. *Water Resour. Res.* **42**, W02419.

Wilby, R., Greenfield, B. & Glenny, C. 1994 A coupled synoptic-hydrological model for climate change impact assessment. *J. Hydrol.* **153**, 265–290.

Wood, A. W., Maurer, E. P., Kumar, A. & Lettenmaier, D. P. 2002 Long range experimental hydrologic forecasting for the eastern U.S. *J. Geophys. Res.* **107** (D20), 4429.

Wood, A. W., Leung, L. R., Sridhar, V. & Lettenmaier, D. P. 2004 Hydrologic implications of dynamical and statistical approaches to downscaling climate model outputs. *Clim. Change* **62**, 189–216.

First received 5 July 2017; accepted in revised form 20 January 2018. Available online 5 March 2018